Drilling fluid solid particle distribution rule analysis in turbodrill thrust ball bearing

Ruyi Gou[1], Xiaodong Zhang[1,2], Wenwu Yang[1]

Abstract. This paper provides a numerical simulation for the two types of turbodrill thrust ball bearing flow field. The Double Fluid Model (DFM) was considered applicable calculation model. The flow field was analyzed by CFX to compare drilling fluid solid phase distribution and volume fraction of solid phase. By comparing the volume fraction and centralized regions of drilling fluid solid particles, the simulation results indicate that the circular arc raceway bearing (CARB) and four point contact bearing (FPCB) solid particle distribution have the similar rules. When solid particles sizes were 2microns and 10 microns, maximum solid phase volume fraction decreased with solid particle size increasing, but increased with solid flow rate increasing. When solid particles sizes were 20 microns and 45 microns, maximum solid phase volume fraction changing rule was completely opposite. The maximum solid phase volume fraction point was located in maximum diameter of FPCB inner ring, and in outer ring raceway centre of CARB. Solid particle distribution rule research is beneficial to bearing lubrication design and to avoid the bearing quick failure.

Key words. Drilling fluid solid particle, thrust ball bearing, turbodrill, distribution rule.

1. Introduction

Turbodrill as an important downhole drilling tool, it is widely used in ultra-deep well, directional well, deep sea drilling [1]. The turbodrill thrust ball bearing is lubricated by drilling fluid, the bearing mainly divided into three forms, such as the circular arc raceway bearing (CARB)[2], four point contact bearing (FPCB)[3] and the polycrystalline diamond sliding thrust bearing[4], this article only study the ball bearing. The thrust bearing of turbodrill used in bottom hole with harsh working condition, such as high speed, high load, downhole high temperature, solid particles as contaminations in drilling fluid lubrication.[5] The solid particles contamination is key impact factor for bearing lubrication and working performance. The solid parti-

---

[1]Workshop 1 - School of Mechatronic Engineering, Southwest Petroleum University, Chengdu, China
[2]Corresponding author:Xiaodong Zhang; e-mail: `zxd123420@126.com`

cle can cause lubrication failure, friction heat generation, bearing surface indentation and fatigue failure.

There is rich of body literature about solid particles influence bearing lubrication and performance. Khader[6]presented an analysis of micropolar fluids between two circular disks, the fluid is laminar flow. The results indicated larger resultant pressures and shear stress occur in lubrication, micropolar fluid is benefit to improve load carrying capacity. Qi [7]investigated the friction behavior of oil-lubricated coated surfaces lubricated with or without sand particles. The DLC coating surfaces lubricated by five type lubricants PAO, PFPE, SO, IL and MAC, the solid-liquid lubrication leads to the wear rates increased by one order of magnitude. The lubrication regimes in Stribeck curve also was strongly affected by solid additives. Qi[8] also studied friction performance of GLC coatings, the GLC coatings were produced by unbalanced magnetron sputtering technique, these coatings have high concentration of Sp2-hybridized carbon. These coatings have synergistic effect and the sand dust particles almost have no influence on the coating friction coefficient and wear resistance. Faisal [9]explored the elliptical-bore journal bearings lubricated with granular in high temperature working condition. The large particle size (2μm) can offer better dynamic performance compared with small particle size (1μm). Using granular as lubricating medium, the bore ellipticity reduces the load-carrying capacity but increases the coefficient of friction. Wongseedakaew [10] considered surface roughness and concentration of solid particles in elastohydrodynamic lubrication(EHL), roughness amplitude and solid particles have influence on film pressure and temperature, the solid particles in Non-Newtonian Lubricant can increases film thickness and decreases friction coefficient. Huang [11] obtained the similar conclusions by spur gears EHL analysis considering solid particles.

In addition drilling fluid is a typical multiphase fluid with non-newtonian rheological behavior. Turbodrill thrust bearing is lubricated by this special lubrication. Many researches focus on the flow model of two phase flow and two phase flow in bearing lubrication. Zhang using the CFD simulation calculated load difference of a test bearing among the two phase model, the results show that the mean cavitation ratio increases with the increasing of speed, eccentricity, and decreasing inlet pressure. Rylander provides a basic theory for hydrodynamic bearings to include the effects of solid particles. It pointed out solid particles causing the increase of friction coefficient is limited by Sommerfeld numbers. Dai developed a model for 2-D lubrication problem involving Newtonian fluid with solid particles, this model using the mixture theory and considering the interaction between particles and fluid. Solid particles influence on slider and journal bearings performance has been discussed, it contains particle slippage and interacting body force. Pereira provided the numerical model describes the solid particles collision and elastic recovery and studied the erosion prediction due to particles in oil and gas transportation at elbow pipe. The above research is mainly focus on multiphase flow or micro lubrication of bearing, So far, there is no report about turbodrill bearing flow field analysis with solid particle. This paper purpose is to analyze solid particle distribution rule and the distribution influence on bearing lubrication. Through the analysis of the maximum solid volume fraction location, solid stranding locations were exactly consistent with field bearing

damaged area. We also obtained the changing rule of solid volume fraction with the particle size and the drilling fluid flow variation. Solid particle distribution research is beneficial to bearing lubrication design and to avoid the bearing quick failure.

2. Simulation model

2.1. Thrust ball bearing model geometry

The model geometry originated from different turbodrill thrust ball bearing, namely, the three-dimensional model of four point contact bearing (FPCB) is shown in Figure 1, the three-dimensional model of circular arc raceway bearing (CARB) is shown in Figure 2.

The FPCB was the first type bearing used in turbodrill and other downhole drilling tools, the CARB was the mature design and widely used in present turbo-drilling. The FPCB or CARB bearing assembly in turbodrill contains 5-10 bearings to withstand the axial load from drill bit and turbine section [3]. The turbine section applies downward hydraulic force on bearing assembly and the drill bit applies upward force on bearing assembly, the upward force is equal to the weight on bit. The radial size of bearing is limited by the borehole size, the bearing is lubricated by drilling fluid, solid particle in drilling fluid can lead uneven load. Meanwhile, the solid particle is easy to cause surface indentation and bearing material fatigue failure when bearing high speed running in drilling process.
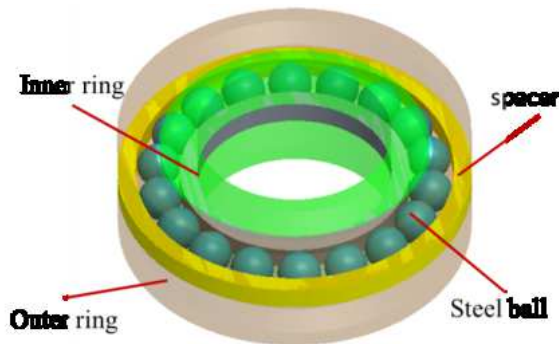

Fig. 1. Three-dimensional model of FPCB

2.2. Governing equations

Due to drilling fluid contains drilling cuttings, weighting materials, chemical additives, etc. Considering of the drilling fluid solid particles suspended particles are micron level, random distribution of solid particles drilling fluid solid phase particle size, volume fraction, density, viscosity can cause complicated flow parameter and Non-Newtonian rheological properties. For this reason, we have considered drilling fluid flow influence on solid particles, but did not take account of the adverse effect
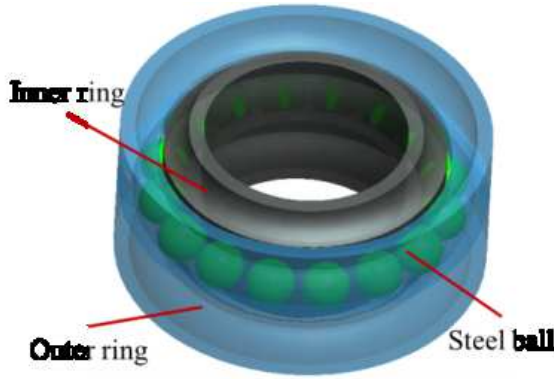
Fig. 2. Three-dimensional model of CARB

of solid particles to drilling fluid. Accordingly, we have adopted Euler method to describe drilling fluid motions, the Double Fluid Model can be expressed as

$$-\frac{\partial}{\partial t}\left(\alpha_k \rho_k\right) + \nabla \cdot \left(\alpha_k \rho_k U_k\right) = 0 \tag{1}$$

$$-\frac{\partial}{\partial t}\left(\alpha_k \rho_k U_k\right) + \nabla \cdot \left(\alpha_k \rho_k U_k U_k\right) = -\nabla \cdot \left(\alpha_k \rho_k\right) + \nabla \cdot \left[\alpha_k \left(\tau_k \tau_k^T\right)\right] + \alpha_k \rho_k F_k \tag{2}$$

$$\sum_{k=1}^{2} \alpha_k = 1 \tag{3}$$

Where k can be replaced by s and f respectively, s is solid phase, f is liquid phase. α_k and ρ_k are phase k concentration and density, respectively. U_k is the flow velocity or solid migration velocity, p_k is compressive stress tensor, τ_k is shear stress tensor. τ_k^T is multiphase pulse stress tensor, F_k is potential force of solid phase or fluid phase, n_k is normal direction of two phase interface. V is phase volume .

Furthermore, drilling fluid solid particles have collision and bounce with thrust bearing components, the interaction between solid and fluid has significant impact on solid particles migration in thrust ball bearing fluid domain, particle collision can adopt elastic recovery coefficient equation to describe:

$$\begin{aligned} e_n &= \frac{u_{p2}}{u_{P1}} = 0.993 - 1.76\theta + 1.56\theta^2 - 0.49\theta^3 \\ e_\tau &= \frac{v_{p2}}{v_{P1}} = 0.998 - 1.66\theta + 2.11\theta^2 - 0.67\theta^3 \end{aligned} \tag{4}$$

Where e_n and e_τ are normal and tangential rebound recovery coefficient, respectively, v_{P1} is normal and tangential velocity before the collision, u_{p2} and v_{p2} are normal and tangential velocity after the collision. θ is solid particle impact angle.

2.3. Computational grid on domain and drilling fluid parameters

Turbodrill is centre symmetric structure, we assume that 18 balls in single pair of bearing are evenly distributed along the circumferential direction, accordingly, the fluid computational domain only one over eighteen of the area to solve flow rule, the calculation model of FPCB and CARB are respectively shown in Figure 3.
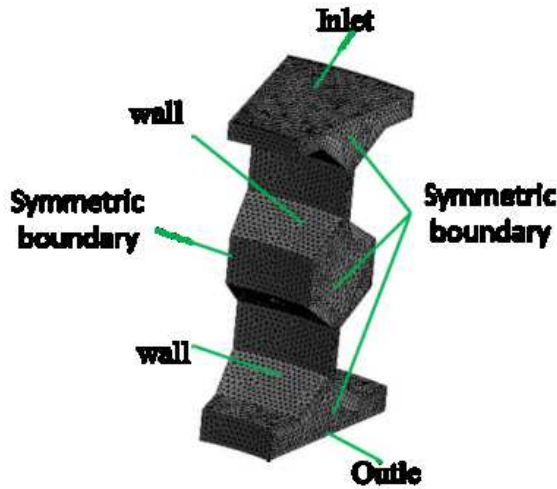

Fig. 3. Fluid computational domain of FPCB

In Figure 3 , the fluid computational domain was meshed by the tetrahedron element, boundary layer adopted hexahedral element, the grid refinement was applied on thrust ball bearing internal wall and contact area. The top surface of computational domain was defined as inlet boundary, the inflow velocity was applied on the inlet boundary. The bottom surface of computational domain was defined as outlet boundary, the reference pressure was applied on the outlet boundary. The right and left side of fluid domain was defined as symmetric boundary, drilling fluid can generate slip on the symmetrical boundaries. In addition to the above mentioned boundary, the rest of the surfaces were defined as walls, drilling fluid can't slip on the wall. However, solid particles can generate slip on all the boundaries and walls. Wall roughness was 5 microns, in drilling process, the smallest size of drilling cuttings was 2 microns.

Drilling solid distribution rule was affected by inlet flow rate, inlet solid phase volume fraction and bearing surface roughness. The parameters drilling fluid through bearing are shown in Table 1. The volume fraction of different size solid particle at the inlet is list in Table 2. The solid particle size is characteristic value of weighting material by centrifuge separation.

vskip 4mm

Table 1. Parameters of drilling fluid

Inlet flow rate (L/s)	Outlet pressure (MPa)	Density (g/cm3)	Viscosity (mPa.s)	weighting material
19~35	10	1.7	66	BaSO4

vskip 4mm

Table 2. Particle size distribution and content percentage of the weighting materials

Particle size(μm)	Water-based weighted drilling fluid
2	12.38%
10	20.16%
20	27.53%
45	39.93%

3. Solid particle distribution in drilling fluid flow field

3.1. The four point contact bearing distribution rule

Drilling fluid flow velocity and pressure distribution in four point contact bearing (FPCB) are shown in Figure 3. Maximum velocity of drilling fluid was in the centre of the annular gap, drilling fluid through the gap flow into the steel ball raceway area, the significant difference of cross section in the annular gap lead the drilling fluid appeared as jet flow, and form vortex area in the centre of the raceway area. The centre flow speed was greater than the velocity on the raceway surface. The pressure distribution in steel ball raceway area has no obvious difference, but the pressure gradually decreased from the inlet boundary to outlet boundary, the pressure drop value was about 0.01 MPa.
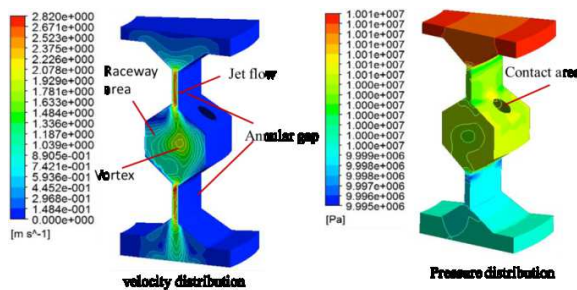

Fig. 4. Flow velocity and pressure distribution in FPCB

The stranded position of solid particles in steel ball raceway area depends on the drilling fluid flow track. The flow track through the FPCB is shown in Figure 6. Due to the steel ball located in the centre of raceway area, drilling fluid chose low resistance flow channel to flow through bearing, thus there was remarkable stream-

ing around steel ball. The drilling fluid flow around the steel ball led to more intense streamline near by the bearing inner ring, as shown in Figure 4 point A. By contrast, point B at the bearing outer ring and point C at the annular gap had sparse streamline. In Figure 3, the velocity variation gradient close to the bearing inner ring was much smaller than velocity variation gradient close to the bearing outer ring. Combined with Figure 3 and Figure 4, most of the solid particles flow around the steel ball along the bearing inner ring with low flow velocity, solid particles were easy to gather at point D, it neared to the bearing inner ring. A small number of solid particles flow around the steel ball along the bearing outer ring. Point E neared located bearing outer ring, it had very low flow velocity. Solid particles were stranded in this area.
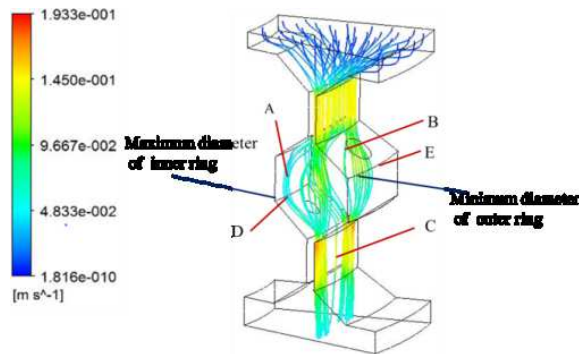
Fig. 5. Drilling fluid flow track through the FPCB

3.2. The circular arc raceway bearing distribution rule

Drilling fluid flow velocity and pressure distribution in circular arc raceway bearing (CARB) are shown in Figure 5. Compared with Figure 3, flow velocity distribution in CARB is similar with FPCB, the maximum velocity, jet flow were generated in CARB had the same location corresponding with FPCB. Because of the mainly differences of two kinds of bearing structure were the raceway curvature and contact form, which had little impact on bearing internal pressure drop. Thus, the pressure drop value in CARB was consistent with FPCB, it was about 0.01MPa. But the vortex area located in point B, it was near the entry of the steel ball raceway area, which produced by the jet flow from the annular gap. The vortex area location, shape and vortex intensity in the CARB was totally different from the FPCB, the vortex motion was much stronger in the CARB than it in the FPCB. Moreover, there was an obvious speed drop zone appears at the wake flow of vortex, the velocity of point A was very small.

The flow track through the CARB is shown in Figure 6, the streamlines indicate the movement track of the drilling fluid in the CARB is similar with the FPCB. But the drilling fluid streamlines around CARB becomes more uniform than streamline in FPCB. The Streamline distribution density in the CARB was much higher than it in the FPCB, but the velocity variation gradient became smaller, which
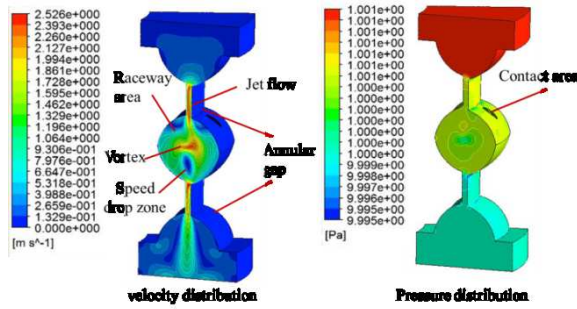
Fig. 6. Flow velocity and pressure distribution in CARB

demonstrates that the CARB has efficient performance of drilling fluid flow. The efficient performance is very favorable to bearing lubrication and cooling, which can effectively avoid solid particle stranding and contact area lubrication starving.

In Figure 8, point A and point B near by the bearing outer ring and the elliptical contact circle, the drilling fluid flow around the steel ball led the vortex form at point A and point B, meanwhile the flow velocity was very low as shown in Figure 7. For these reasons, the point A and point B tended to generate solid particles stranding.
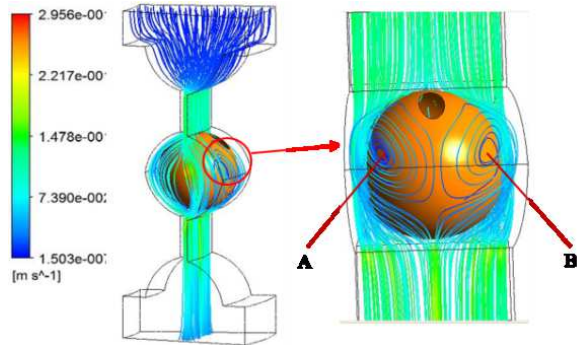

Fig. 7. Drilling fluid flow track through the CARB

4. Drilling fluid properties influence on solid particle volume fraction

4.1. Solid phase volume fraction of raceway surface in FPCB

According to the different drilling fluid flow rate and 4 kinds of particle size, solid particle size and flow rate influence on solid phase volume fraction of FPCB raceway surface are shown in Table 3.

By comparing the contours of different solid particle size, when solid particles

sizes were 2microns and 10 microns, the simulation results show that maximum solid phase volume fraction of raceway surface decreased with solid particle size increasing. This is because the solid particles size were larger than the bearing surface roughness, the smaller possibility of stranded in the bearing surface, when solid particle size less than 5 microns, these tiny solid particles were prone to be stranded in the rough peak of raceway surface. But when solid particles sizes were 20 microns and 45 microns, maximum solid phase volume fraction of raceway surface increased with solid particle size increasing. This is because the larger size solid particles had poor mobility along with drilling fluid, the larger solid particles were easily to strand by the effect of vortex.

By comparing the contours of different fluid flow rate, when the solid particle size was 2 microns or 10 microns, the solid phase volume fraction of raceway surface decreased with flow rate increasing, because when the drilling fluid flow rate was 35L/s, it had stronger solid particles carrying capacity. The solid particles sizes less than 10 microns, quality of particle was very small, so solid particles were washed downward to outlet boundary. However, when solid particles sizes were 20 microns or 45 microns, the solid phase volume fraction had the opposite pattern. In spite of drilling fluid particle carrying capacity increased with flow rate, the vortex effect was also more intense, the 20 microns or 45 microns had low flow velocity, the larger solid particles would be stranded in the bearing. The maximum volume of 45 microns was about 32% higher than 20microns. The stranding locations of solid particles were same with maximum volume fraction points.

By comparing the solid particle volume fraction in Table 3, with the same flow rate condition, solid particle size varied from 2microns to 45microns, the maximum solid phase volume fraction points on bearing inner ring contact surface are shown as point A and point B in Table 3. Point A was located at wake flow of contact area on inner ring, point B was located at maximum outer diameter of the inner ring. With the solid size increasing, the maximum value of solid phase volume fraction migrated from point A to point B.

vskip 4mm

Table 3. Solid phase volume fraction of raceway surface in FPCB
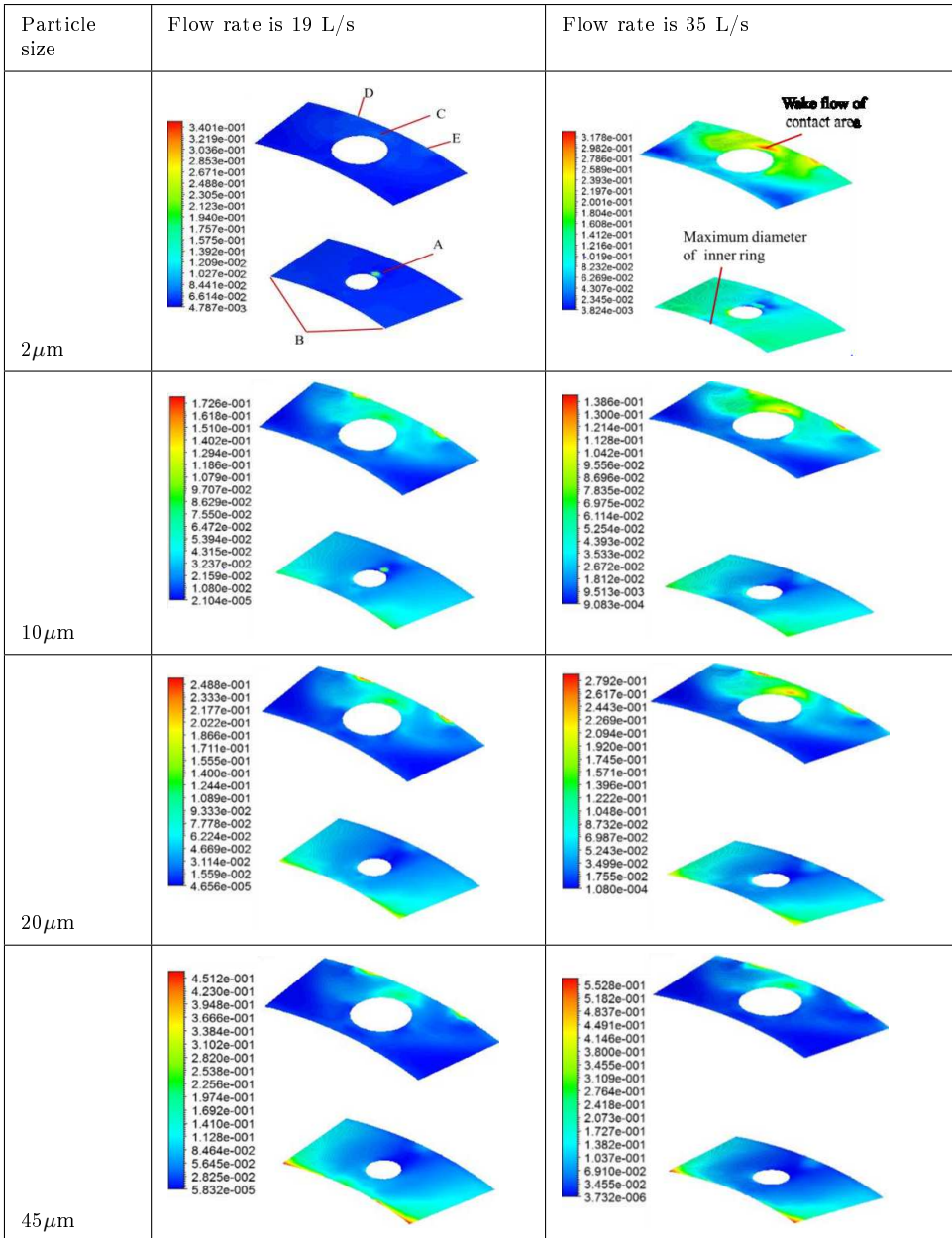
Particle size	Flow rate is 19 L/s	Flow rate is 35 L/s
2μm		
10μm		
20μm		
45μm		

The maximum solid phase volume fraction points on bearing outer ring contact surface are shown as point C, point D and point E. Point C was located at wake flow of contact area on outer ring, point D and point E were located at minimum inner diameter of the outer ring. With the solid size increasing, the maximum volume fraction of solid phase migrated from point C to point D and point E.

The results demonstrate that the FPCB maximum volume fraction points are located at maximum diameter of the inner ring and minimum outer diameter of outer ring, which is consistent with bearing failure mode in field application. The damaged inner bearing of FPCB is shown in Figure 9. The material spalling occurs in maximum diameter of inner ring, its location is consistent with maximum volume fraction point B in Table 3.


Fig. 8. The damaged inner ring of FPCB after field application

4.2. Solid phase volume fraction of raceway surface in CARB

Solid particle size and flow rate influence on solid phase volume fraction of CARB raceway surface are shown in Table 4.By comparing the contours of different solid particle size and different fluid flow rate in Table 4, the change rule of maximum solid phase volume fraction is same with FPCB. Under the same flow rate, the maximum solid phase volume fraction increases with solid particle size increasing. When the flow rate increased, the 2 microns or 10 microns solid particle maximum volume fraction decreased, on the contrary, the 20 microns or 45 microns solid particle maximum volume fraction increased.

vskip 4mm

Table 4. Solid phase volume fraction of raceway surface in CARB
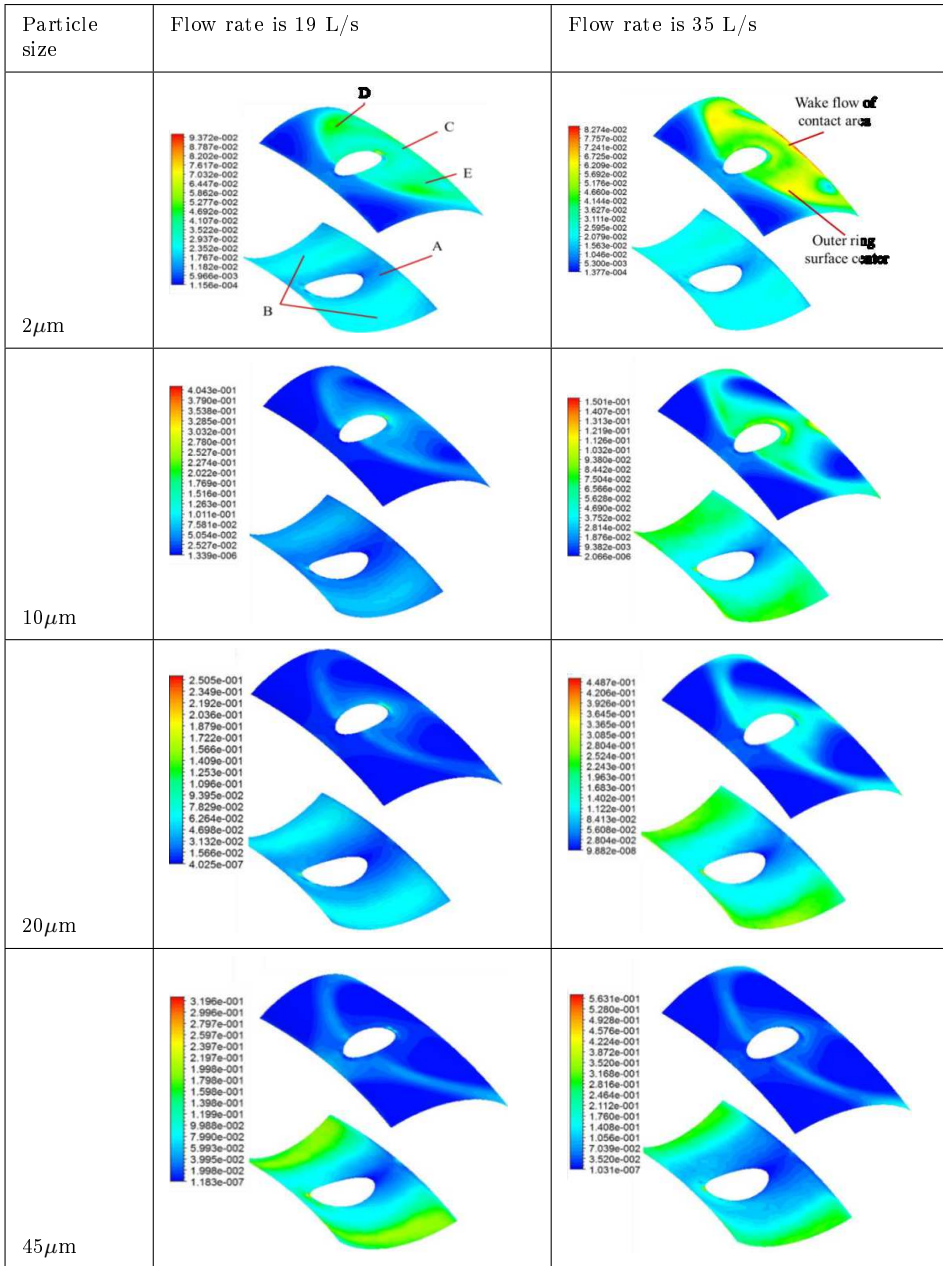
Particle size	Flow rate is 19 L/s	Flow rate is 35 L/s
2μm		
10μm		
20μm		
45μm		

The maximum volume fraction of solid phase point migration direction is opposite to FPCB completely. Solid particles in CARB are prone to stranded at outer ring surface. Thus, the raceway surface centre of CARB strands more solid particles than other area of raceway surface, the drilling fluid starving condition, poor lubrication, raceway surface indentation and fatigue crack will be concentrated in the area. The

simulation results coincide with CARB failure mode, the failure CARB after field application is shown in Figure 10. The fatigue crack on outer ring raceway surface centre, its location is consistent with maximum volume fraction point D and point E in Table 4.

In Table 4, the maximum solid phase volume fraction points on bearing outer ring contact surface are shown as point C, point D and point E. Point C is located at wake flow of contact area, point D and point E are located at outer ring surface centre. With the solid size increasing, the maximum volume fraction of solid phase point D and point E migrate to point C, this is caused by the vortex effect is improved. The stranding location depends on the centre of the vortex motion.

This maximum volume fraction of solid phase point migration direction is opposite to FPCB completely. Solid particles in CARB are prone to stranded at outer ring surface. Thus, the raceway surface centre of CARB strands more solid particles than other area of raceway surface, the drilling fluid starving condition, poor lubrication, raceway surface indentation and fatigue crack will be concentrated in the area. The simulation results coincide with CARB failure mode, the failure CARB after field application is shown in Figure 10. The fatigue crack on outer ring raceway surface centre, its location is consistent with maximum volume fraction point D and point E in Table 4.

Fatigue crack on on outer ring raceway surface center

Fig. 9. The damaged outer ring CARB after field application

5. Conclusions

Solid particle distribution in drilling fluid flow field shows that the FPCB and the CARB have similar distribution rule, both of them had jet flow in the centre of the annular gap and vortex in centre of the raceway area. But vortex of CARB was closer to the entry of the steel ball raceway area, and the CARB had an obvious speed drop zone appears at the wake flow of vortex.

With the same boundary conditions, the streamlines of the FPCB was sparse, but streamline of the CARB was very intensive, moreover, the streamline of the CARB had vortex area locating in outer ring raceway surface centre.

The maximum volume fraction of solid phase changing rules for the FPCB and the CARB have the same trends. When solid particles sizes were 2microns and 10 microns, maximum solid phase volume fraction decreased with solid particle size increasing, but increased with solid flow rate increasing. When solid particles sizes were 20 microns and 45 microns, maximum solid phase volume fraction changing rule was completely opposite.

The maximum solid phase volume fraction point locations are consistent with bearing failure location, the FPCB was maximum diameter of inner ring. The CARB was outer ring raceway surface centre.

References

[1] V. MOKARAMIAN, V. RASOULI, G. CAVANOUGH: *A hydraulic specific energy performance indicator for coiled tube turbodrilling.* U.s.rock Mechanics/geomechanics Symposium (2012).

[2] F. D. XU, B. Z. HUA: *Construction optimum and analysis on capacity of support loads of three thrust bearings used in turbodrill.*Oil Field Equipment *33* (2004), 47–49.

[3] T. N. SEXTON, C. H. COOLEY: *Polycrystalline diamond thrust bearings for downhole oil and gas drilling tools.* Wear *267* (2009), 1041–1045.

[4] F. D. XU, B. Z. HUA: *Mechanism of average distribution of load for four points contact ball bearing in the turbodrill.* Mining & Processing Equipment (1999), 19–20.

[5] M. S. KHADER, R. I. VACHON: *Theoretical Effects of Solid Particles in Hydrostatic Bearing Lubricant.* J. of Tribology *95* (1973), 104.

[6] J. QI, L. WANG, F. YAN, Q. XUE: *The tribological performance of DLC-based coating under the solid–liquid lubrication system with sand-dust particles.* Wear *297* (2013) 972–985.

[7] J. QI, H. LIU, Y. LUO, D. ZHANG, Y. WANG: *Influences of added sand-dust particles on the tribological performance of graphite-like coating under solid-liquid lubrication.* Tribology International *71* (2014), 69–81.

[8] FAISAL, RAHMANI, JAYANTA, DUTT, PANDEY: *Performance behaviour of elliptical-bore journal bearings lubricated with solid granular particulates.* Particuology *4* (2016), 51–60.

[9] K. WONGSEEDAKAEW, J. PANICHAKORN: *Effect of Solid Particle on Rough Thermo-Elastohydrod-ynamic Lubrication with Non-Newtonian Lubricant.* Advanced Materials Research *1044* (2014), 305–309.

[10] X. HUANG, Y. WANG: *Transient elastohydrodynamic lubrication analysis of spur gears running-in considering effects of solid particles and surface roughness.* Industrial Lubrication and Tribology *68*, (2016), 183–190.

[11] C. ZHANG, J. YANG, R. GUO, D. SUN: *Simulation of journal bearing flow field using computational fluid dynamics two phase flow theory.* Proceedings of the Csee *30*, (2010), 80–84.